

Investigation of possible hadronic flow in $\sqrt{s_{NN}} = 5.02$ TeV p -Pb collisions

You Zhou,^{1,2,*} Xiangrong Zhu,¹ Pengfei Li,¹ and Huichao Song^{1,3,4,†}

¹*Department of Physics and State Key Laboratory of Nuclear Physics and Technology, Peking University, Beijing 100871, China*

²*Niels Bohr Institute, University of Copenhagen, Blegdamsvej 17, 2100 Copenhagen, Denmark*

³*Collaborative Innovation Center of Quantum Matter, Beijing 100871, China*

⁴*Center for High Energy Physics, Peking University, Beijing 100871, China*

(Received 24 March 2015; revised manuscript received 18 May 2015; published 12 June 2015)

Using the ultrarelativistic quantum molecular dynamics (UrQMD) model, we investigate azimuthal correlations in p -Pb collisions at $\sqrt{s_{NN}} = 5.02$ TeV. Comparison with the experimental data shows that UrQMD cannot reproduce the multiplicity dependence of two- and four-particle cumulants, especially the transition from positive to negative values of $c_2\{4\}$ in high-multiplicity events, which has been taken as experimental evidence of collectivity in p -Pb collisions. Meanwhile, UrQMD cannot describe the differential elliptic flow $v_2(p_T)$ of all charged hadrons at various multiplicity classes. These discrepancies show that the simulated hadronic p -Pb systems cannot generate enough collective flow as observed in experiment, the associated hadron emissions are largely influenced by nonflow effects. However, the characteristic $v_2(p_T)$ mass ordering of pions, kaons, and protons is observed in UrQMD, which is the consequence of hadronic interactions and not necessarily associated with strong fluid-like expansions.

DOI: [10.1103/PhysRevC.91.064908](https://doi.org/10.1103/PhysRevC.91.064908)

PACS number(s): 25.75.Ld, 25.75.Gz, 24.10.Lx

I. INTRODUCTION

The relativistic heavy ion collisions at Relativistic Heavy Ion Collider (RHIC) and the Large Hadron Collider (LHC) have provided strong evidences for the creation of the quark-gluon plasma (QGP) [1–4]. One of the crucial observables is the azimuthal anisotropy of the transverse momentum distribution for produced hadrons [5]. As a signature of the collective flow, it provides important information on the equation of state (EoS) and the transport properties of the QGP [6–11]. Usually, the anisotropy is characterized by the Fourier flow coefficients [12]

$$v_n = \langle \cos[n(\varphi - \Psi_n)] \rangle, \quad (1)$$

where φ is the azimuthal angle of the emitted hadrons, Ψ_n is the n th-order participant (symmetry) plane angle and $\langle \rangle$ denotes an average of all particles in all events. The second Fourier flow-coefficient v_2 is called elliptic flow, which is associated with the initial elliptic overlap region of the two colliding nuclei. In past decades, most attention had been paid to the elliptic flow v_2 , which was systematically measured and studied at the Super Proton Synchrotron (SPS) [13], RHIC [14–17], and the LHC [18–20] (for a summary, please also refer to Refs. [21,22]). More recently, it was realized that the higher-order flow coefficients are equally important, because they provide information on the fluctuating initial profiles of the created QGP [23–37].

The measurements of azimuthal correlations in $\sqrt{s_{NN}} = 5.02$ TeV p -Pb collisions at the LHC were originally aimed to provide reference data for the high-energy Pb-Pb collisions, especially on the cold-nuclear-matter effects. However, a large amount of unexpected collective behavior has been

discovered by the ALICE, ATLAS, and CMS collaborations. For instance, a symmetric double-ridge structure on both the near- and away-side has been observed in high-multiplicity p -Pb collisions by the ALICE Collaboration [38]. In addition, the CMS Collaboration has showed compatible results between multiparticle (including four, six, and eight particles) and all-particle correlations with Lee–Yang zeros (LYZ) [39], which corresponds to $v_2\{4\} \approx v_2\{6\} \approx v_2\{8\} \approx v_2\{\text{LYZ}\}$ [40] (these results were confirmed by the ATLAS [41] and ALICE collaborations [42]). Recently, the measurements of azimuthal correlations were extended to identified hadrons [43,44]. A v_2 mass-ordering feature, which says that the differential elliptic flow at the low-transverse-momentum region monotonically increases with the decrease of hadron mass, has been observed among pions, kaons, and protons in high-multiplicity events [43]. Similarly, the CMS Collaboration found the mass ordering between K_S^0 and $\Lambda(\bar{\Lambda})$, which showed that the v_2 of K_S^0 is larger than that of $\Lambda(\bar{\Lambda})$ at lower p_T , followed by a crossing at $p_T \sim 2$ GeV [44]. Many of these experimental measurements have been semiquantitatively described by $(3+1)$ -dimensional hydrodynamic simulations from several groups [45–49], which support the experimental claim that large collective flow has been developed in small p -Pb systems.

In Au-Au or Pb-Pb collisions at RHIC and the LHC, the collective flow mainly develops in the QGP phase since the QGP fireball has a sufficiently long lifetime to develop the momentum anisotropy until the saturation is almost reached [6,50,51]. Meanwhile, a certain amount of collective flow is further accumulated in the hadronic stage through the microscopic rescatterings, which leads to the v_2 mass ordering among various hadron species [52–55]. Compared with Au-Au or Pb-Pb collisions, the smaller systems created in p -Pb collisions have much shorter lifetime. As a result, the momentum anisotropy is not likely to reach saturation even if the QGP has been created. The measured azimuthal correlations in p -Pb collisions might be largely influenced

*you.zhou@cern.ch

†huichaosong@pku.edu.cn

by the hadronic evolution. On the other hand, non-flow effects (e.g., from hadron resonance decays) are significantly enhanced for a smaller system with much lower particle yields, which also contribute to two-particle correlations [21].

With an assumption of early thermalization for the p -Pb systems created, hydrodynamics simulates the evolution of both QGP and hadronic phases and associates the azimuthal correlations of all charge and identified hadrons with the collective expansion of the systems [45–49]. In this paper, we assume that the high-energy p -Pb collisions do not reach the threshold of the QGP formation, only pure hadronic systems are produced. We utilize the hadron cascade model called the ultrarelativistic quantum molecular dynamics (UrQMD) model [56–58] to simulate the evolution of the hadronic matter and then study the azimuthal correlations of the final hadrons produced. Our research focuses on two aspects: (1) investigating whether pure hadronic interactions could generate the observed flow signatures in high-multiplicity events; (2) studying the mass ordering of two-particle correlations in pure hadronic p -Pb systems.

The paper is organized as follows: Section II briefly introduces the UrQMD model. Section III outlines the two- and four-particle Q -cumulant method. Section IV compares experimental measurements with the UrQMD calculations on two- and four-particle azimuthal correlations, including centrality dependence and transverse momentum dependence. Section V summarizes and concludes this work.

II. ULTRARELATIVISTIC QUANTUM MOLECULAR DYNAMICS HADRON CASCADE MODEL

UrQMD is a microscopic transport model to describe hadron-hadron, hadron-nucleus, and nucleus-nucleus collisions at relativistic energies, based on the Boltzmann equations for various hadron species [56–58]. It has successfully described the soft physics at the energies of the BNL Alternating Gradient Synchrotron and the SPS, where the created systems are dominated by strongly interacting hadrons.

In UrQMD, the initial hadron productions are modeled via the excitation and fragmentation of strings. For higher collision energies above $\sqrt{s_{NN}} = 10$ GeV, the PYTHIA mode [59] is implemented to describe the hard processes and the related hadron productions. The classical trajectories of the produced hadrons are then simulated through solving a large set of Boltzmann equations with flavor-dependent cross sections. In the later version, UrQMD contains 55 baryon and 32 meson species with masses up to 2.25 GeV, supplemented

TABLE I. Event class determination in UrQMD according to the number of all charged hadrons within $|\eta| < 1.0$.

Event class	$N_{\text{ch}} (\eta < 1.0)$
0%–5%	>72
5%–10%	60–72
10%–20%	47–60
20%–40%	38–47
40%–60%	17–23
60%–100%	<17

TABLE II. Event class determination in UrQMD according to the number of charged hadrons within $2.8 < \eta < 5.1$.

Event class	$N_{\text{ch}} (2.8 < \eta < 5.1)$
0%–20%	>88
20%–40%	54–88
40%–60%	30–54
60%–80%	13–30
80%–100%	≤ 13

by the corresponding antiparticles and isospin-projected states [58]. The elementary cross sections in the collision terms are either fit from the experimental data or calculated via models, e.g., a modified additive quark model (AQM). For two closely propagating hadrons, whether a collision happens is determined by a critical distance associated with the related cross section. When all elastic and inelastic collisions cease and all unstable hadrons have decayed into stable hadrons, the system is considered to reach kinetic freeze-out. UrQMD then outputs the momentum and position information of the final hadrons produced.

In this paper, we implement UrQMD version 3.4 to simulate the evolution of the assumed hadronic systems created in high-energy p -Pb collisions. The simulations are executed in the equal-speed system of two colliding nucleons with $\sqrt{s_{NN}} = 5.02$ TeV. Correspondingly, the output information for the final hadrons produced are defined in the center-of-mass frame. In order to compare with the experimental data in the laboratory frame, we make a transformation between the center-of-mass frame and the laboratory frame, which shifts the rapidity by 0.465. Following the related experimental papers [42,43,60],

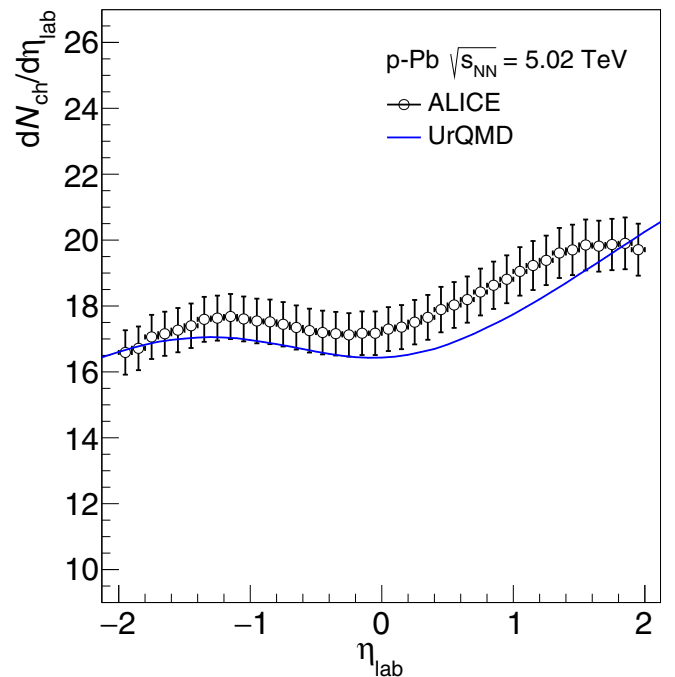


FIG. 1. (Color online) Pseudorapidity density of all charged hadrons in minimum bias p -Pb collisions at $\sqrt{s_{NN}} = 5.02$ TeV, measured by ALICE [61] and calculated from UrQMD.

the UrQMD outputs are divided into several multiplicity classes, determined by the number of all charged hadrons N_{ch} within a pseudorapidity range $|\eta| < 1$ or $2.8 < \eta < 5.1$. The N_{ch} values in these two centrality definitions are shown Tables I and II. The pseudorapidity density of all charged hadrons as a function of pseudorapidity in minimum-bias p -Pb collisions is presented in Fig. 1.

III. ANALYSIS METHOD AND DEFINITIONS

In this paper, the azimuthal correlations are calculated using the two- and four-particle Q -cumulant methods [62,63], which were used in experiment at RHIC [64] and the LHC [18,33,40,65]. In this method, both two- and multiparticle azimuthal correlations are analytically expressed in terms of a Q vector, which is defined as

$$Q_n = \sum_{i=1}^M e^{in\phi_i}, \quad (2)$$

where M is the multiplicity of the reference flow particles (RFPs) and ϕ is their azimuthal angle. The single-event average two- and four-particle azimuthal correlations can be calculated via

$$\begin{aligned} \langle 2 \rangle &= \frac{|Q_n|^2 - M}{M(M-1)}, \\ \langle 4 \rangle &= \frac{|Q_n|^4 + |Q_{2n}|^2 - 2\text{Re}[Q_{2n}Q_n^*Q_n^*]}{M(M-1)(M-2)(M-3)} \\ &\quad - 2 \frac{2(M-2)|Q_n|^2 - M(M-3)}{M(M-1)(M-2)(M-3)}, \end{aligned} \quad (3)$$

where $\langle \rangle$ stands for the average over all particles in a single event.

The two- and four-particle cumulants could be achieved as

$$c_n\{2\} = \langle \langle 2 \rangle \rangle, \quad c_n\{4\} = \langle \langle 4 \rangle \rangle - 2\langle \langle 2 \rangle \rangle^2, \quad (4)$$

here $\langle \langle \rangle \rangle$ denotes the average over all particles over all events.

In order to proceed with the calculation of the differential flow of the particles of interest (POIs), the p_n and q_n vectors for specific kinematic range and/or for specific hadron species are needed:

$$p_n = \sum_{i=1}^{m_p} e^{in\phi_i}, \quad q_n = \sum_{i=1}^{m_q} e^{in\phi_i}, \quad (5)$$

where m_p is the total number of particles labeled as POIs, and m_q is the total number of particles tagged both as RFP and POI.

The single-event average differential two- and four-particle azimuthal cumulants are calculated as

$$\begin{aligned} \langle 2' \rangle &= \frac{p_n Q_n^* - m_q}{m_p M - m_q}, \\ \langle 4' \rangle &= [p_n Q_n Q_n^* Q_n^* - q_{2n} Q_n^* Q_n^* - p_n Q_n Q_{2n}^* \\ &\quad - 2M p_n Q_n^* - 2m_q |Q_n|^2 + 7q_n Q_n^* - Q_n q_n^* \\ &\quad + q_{2n} Q_{2n}^* + 2p_n Q_n^* + 2m_q M - 6m_q] \\ &\quad \div [(m_p M - 3m_q)(M-1)(M-2)]. \end{aligned} \quad (6)$$

For detectors with uniform azimuthal acceptance the differential two- and four-particle cumulants are given by

$$d_n\{2\} = \langle \langle 2' \rangle \rangle, \quad d_n\{4\} = \langle \langle 4' \rangle \rangle - 2\langle \langle 2' \rangle \rangle \langle \langle 2 \rangle \rangle. \quad (7)$$

Finally, the estimated differential flow $v_2(p_T)$ from two- and four-particle correlations are given by

$$v_n\{2\}(p_T) = \frac{d_n\{2\}}{\sqrt{c_n\{2\}}}, \quad v_n\{4\}(p_T) = -\frac{d_n\{4\}}{(-c_n\{4\})^{3/4}}. \quad (8)$$

Unfortunately, the v_n obtained from the two-particle Q cumulant contains contributions from so-called non-flow effects, which are additional azimuthal correlations between the particles due to, e.g., resonance decays, jet fragmentation, and Bose-Einstein correlations. They can be suppressed by appropriate kinematic cuts. For instance, one can introduce a pseudorapidity gap between the particles in the two-particle Q cumulant method [65]. Accordingly, the whole event is divided into two subevents, A and B , which are separated by a $|\Delta\eta|$ gap. This modifies Eq. (3) to

$$\langle 2 \rangle_{\Delta\eta} = \frac{Q_n^A Q_n^{B*}}{M_A M_B}, \quad (9)$$

where Q_n^A and Q_n^B are the flow vectors from subevents A and B , and M_A and M_B are the corresponding multiplicities.

The two-particle Q cumulant with a $|\Delta\eta|$ gap is given by

$$c_n\{2, |\Delta\eta|\} = \langle \langle 2 \rangle \rangle_{\Delta\eta}. \quad (10)$$

For the calculations of differential flow with a pseudorapidity gap, there is no overlap of POIs and RPs if we select RPs from one subevent and POIs from the other. This modifies Eqs. (6) to

$$\langle 2' \rangle_{\Delta\eta} = \frac{p_{n,A} Q_{n,B}^*}{m_{p,A} M_B}, \quad (11)$$

and we get the differential two-particle cumulant as

$$d_n\{2, |\Delta\eta|\} = \langle \langle 2' \rangle \rangle_{\Delta\eta}. \quad (12)$$

Finally, the differential flow from the two-particle cumulant can be obtained by inserting the two-particle reference flow (with an η gap) to the differential two-particle cumulant:

$$v_n\{2, |\Delta\eta|\}(p_T) = \frac{d_n\{2, |\Delta\eta|\}}{\sqrt{c_n\{2, |\Delta\eta|\}}}. \quad (13)$$

In this paper, the second and third Fourier flow-coefficients are evaluated by using the above equations and setting $n = 2$ and 3, respectively.

IV. RESULTS AND DISCUSSIONS

This section mainly investigates the second and third Fourier flow coefficients with cumulants in p -Pb collisions at $\sqrt{s_{NN}} = 5.02$ TeV. Before studying the two-particle and four-particle correlations, it is important to check the single hadron information. Figure 1 plots the pseudorapidity density of all charged hadrons $dN_{\text{ch}}/d\eta$ in minimum bias p -Pb collisions. In general, UrQMD roughly describes the forward-backward asymmetry of the $dN_{\text{ch}}/d\eta$ curve within $|\eta| < 2$. At midrapidity, $dN_{\text{ch}}/d\eta$ from UrQMD are close to the ALICE

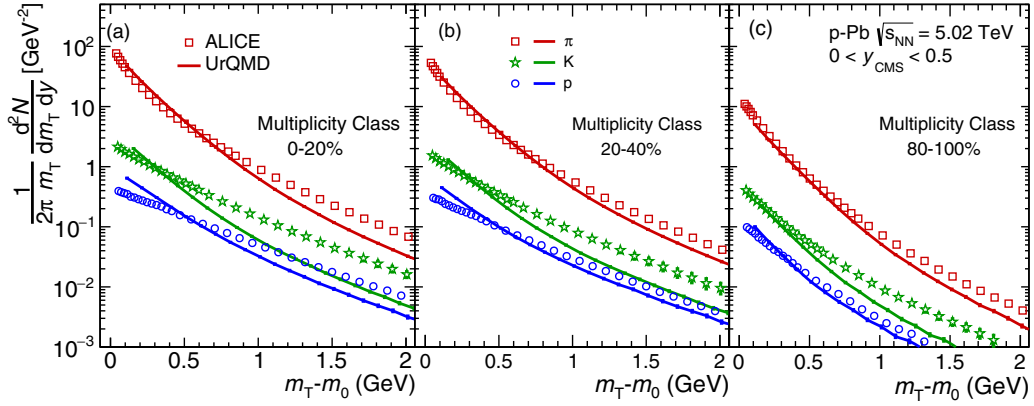


FIG. 2. (Color online) The m_T spectra of pions, kaons, and protons in p -Pb collisions at $\sqrt{s_{NN}} = 5.02$ TeV measured by ALICE [60] and calculated from UrQMD. Here the multiplicity class determination in UrQMD is based on Table II.

measurements, but about 5% lower than the experimental values.

Figure 2 plots the m_T spectra of pions, kaons, and protons in high-energy p -Pb collisions. It is generally believed that, in the absence of radial flow, m_T spectra as a function of $m_T - m_0$ [m_0 stands for the rest mass of the hadron and $m_T = (p_T^2 + m_0^2)^{1/2}$] satisfies the m_T scaling, where the slopes of the spectra are independent of hadron species [66]. Such m_T scaling has been observed in p - p collisions at $\sqrt{s_{NN}} = 200$ GeV [66,67]. In heavy-ion collisions at the SPS energies and above, the m_T scaling is broken, which provides evidence for the development of strong radial flow in hot QCD systems [66–70].

In high-energy p -Pb collisions at $\sqrt{s_{NN}} = 5.02$ TeV, the ALICE measurements in Fig. 2 show that m_T scaling is broken at 0%–20% and 20%–40% multiplicity classes where the measured protons spectra are flatter than kaons ones.¹ This provides evidence for the development of radial flow in high-multiplicity events. The UrQMD calculations in Fig. 2 also present a weak breaking of the m_T scaling, but show steeper spectra for pions, kaons, and protons. Meanwhile, UrQMD produces much fewer kaons, leading to even larger deviations for the kaon spectra when compared with the ALICE data.

To further evaluate the breaking of the m_T scaling, we implement the Boltzmann distribution function $\frac{dN}{m_T dm_T} \propto$

¹The pion spectra are largely influenced by resonance decays at lower $m_T - m_0$, which break the pion’s m_T scaling even for the case without radial flow.

TABLE III. Effective temperatures extracted from the m_T spectra of ALICE. The Boltzmann-function fitting ranges are $0.5 < p_T < 1.0$ for pions, $0.2 < p_T < 1.5$ for kaons, and $0.3 < p_T < 3.0$ for protons.

T_{eff} (GeV)	π	K	p
0%–20%	0.228	0.234	0.198
20%–40%	0.298	0.295	0.222
80%–100%	0.395	0.389	0.281

$\exp(-\frac{m_T}{T_{\text{eff}}})$ to fit the m_T spectra of pions, kaons, and protons for ALICE and UrQMD. The extracted effective temperatures are summarized in Tables III and IV. For each chosen centralities, T_{eff} varies with the hadron mass m_0 , directly showing the breaking of the m_T scaling for both ALICE and UrQMD. The different slopes of the m_T spectra between theory and experiment also indicate that the assumed hadronic p -Pb systems could not produce the amount of radial flow as observed in experiment.²

With brief investigations of the single-hadron data, we now focus on studying azimuthal correlations in high-energy p -Pb collisions. Figure 3 presents the centrality dependence of the two-particle cumulant of the second Fourier flow coefficient $c_2\{2\}$, calculated from UrQMD hadron cascade model (left) and measured by the ALICE collaboration (right). For various pseudorapidity gaps, $c_2\{2\}$ from UrQMD exhibit a decreasing trend from peripheral (low-multiplicity events) to central collisions (high-multiplicity events), which agrees with the expectation of the azimuthal correlations not associated with

²We also find that the blast-wave model [71] that describes the evolving system with an average flow velocity and a kinetic freeze-out temperature can fit the ALICE spectra with $\langle\beta\rangle = 0.525$, $T_{\text{kin}} = 0.146$ GeV; $\langle\beta\rangle = 0.476$, $T_{\text{kin}} = 0.15$ GeV, and $\langle\beta\rangle = 0.249$, $T_{\text{kin}} = 0.168$ GeV for 0%–20%, 20%–40%, and 80%–100% centralities [72], indicating the development of radial flow in the created p -Pb systems. However, the blast-wave model fails to describe the UrQMD results [72], which illustrates that the slight breaking of the m_T scaling in UrQMD is not due to the radial flow but is caused by other effects.

TABLE IV. Effective temperatures extracted from the m_T spectra of UrQMD. The Boltzmann-function fitting ranges are $0.3 < p_T < 0.9$ for pions, $0.2 < p_T < 1.1$ for kaons, and $0.25 < p_T < 1.5$ for protons.

T_{eff} (GeV)	π	K	p
0%–20%	0.161	0.163	0.155
20%–40%	0.189	0.190	0.170
80%–100%	0.245	0.234	0.175

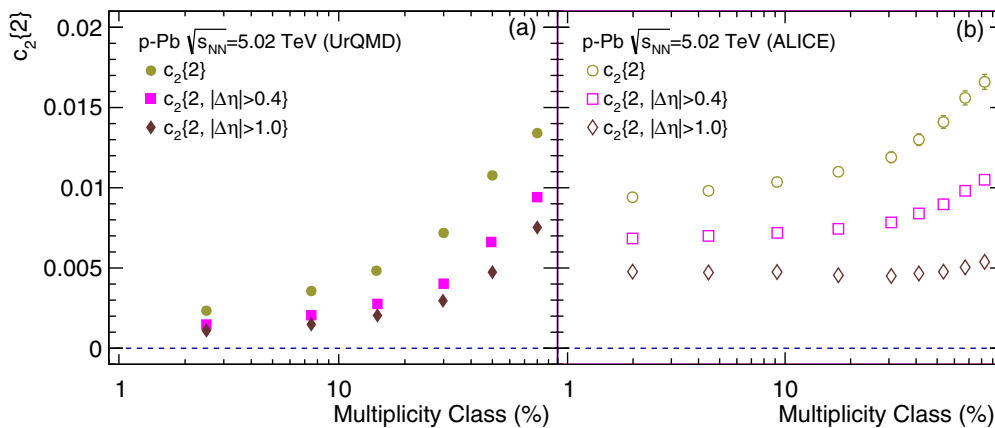


FIG. 3. (Color online) $c_2\{2\}$ of all charged hadrons in p -Pb collisions at $\sqrt{s_{NN}} = 5.02$ TeV, calculated UrQMD (left) and measured by ALICE (right) [42]. The circle, square, and diamond markers represent various pseudorapidity gap cuts without η gap, with gap $|\Delta\eta| > 0.4$, and $|\Delta\eta| > 1.0$, respectively. Here the multiplicity class determination in UrQMD is based on Table I.

the symmetry plane; the so-called non-flow effects. As the pseudorapidity gap increases, the magnitudes of $c_2\{2\}$ become weaker for both ALICE and UrQMD, which illustrates that non-flow effects, usually few-particle correlations from resonance decays and jets, are suppressed by a large pseudorapidity gap. When the pseudorapidity gap $|\Delta\eta|$ is larger than 1.0, $c_2\{2\}$ from ALICE show much weaker centrality dependence, which is suggested as one of the hints for collective expansion in the created p -Pb systems. However, $c_2\{2\}$ from UrQMD still present a strong centrality dependence for $|\Delta\eta| > 1.0$, showing a typical non-flow behavior. Usually, the non-flow effects between two-particle correlations, denoted as δ_n , behave as $\delta_n \sim 1/M$ where M is the multiplicity. The decreasing trend of $c_2\{2\}$ with the increase of multiplicity indicates that UrQMD hadronic expansion could not generate sufficient flow in a small p -Pb system; non-flow effects are still pretty large even for the case with a large pseudorapidity gap cut $|\Delta\eta| > 1.0$.

To better understand the hadronic systems simulated by UrQMD, we investigate the four-particle cumulant of the second Fourier flow coefficient $c_2\{4\}$, which is equal to $-v_2\{4\}^4$ and is expected to be less sensitive to non-flow effects. Figure 4 plots the centrality dependence of $c_2\{4\}$ of all charged hadrons in p -Pb collisions at $\sqrt{s_{NN}} = 5.02$ TeV. Both the UrQMD and ALICE results show that $c_2\{4\}$ increase with the decrease of multiplicity from semicentral to peripheral collisions. For the most-central collisions ($<10\%$), $c_2\{4\}$ from ALICE exhibits a transition from positive to negative values, indicating the creation of flow-dominated systems in the high-multiplicity events. However, $c_2\{4\}$ from UrQMD keeps positive for all available multiplicity classes, including the most central collisions. As a result, real values of $v_2\{4\}$ cannot be extracted in UrQMD for all centrality bins. This comparison further illustrates the difference between the p -Pb systems created in experiment and simulated by UrQMD. The hadron emissions from UrQMD are largely influenced by nonflow effects. Without the contributions from the initial stage and/or the QGP phase, the measured flow-like four-particle correlations in high-multiplicity events cannot

be reproduced by a microscopic transport model with only hadronic scatterings and decays.

In Figure 5, we further study the two-particle azimuthal correlations for the third Fourier flow-coefficient $c_3\{2\}$. The UrQMD calculations and the ALICE measurements with various pseudorapidity gaps are respectively shown in the left and right panels of Fig. 5. Similar to $c_2\{2\}$ in Fig. 3, $c_3\{2\}$ also decreases with the increase of $|\Delta\eta|$. For the ALICE measurement, $c_3\{2\}$ stays positive for all pseudorapidity gaps, which leads to real values of triangular flow $v_3\{2\}$ ($v_3\{2\} = \sqrt{c_3\{2\}}$) as measured in Ref. [42]. Considering that non-flow effects are largely suppressed by a large pseudorapidity gap, the measured $c_3\{2\}$ at $|\Delta\eta| > 1.0$ (and the associated triangular flow $v_3\{2\}$) is possibly caused mainly by collective expansion and reflects initial-state fluctuations of the p -Pb systems. In contrast, $c_3\{2\}$ from UrQMD becomes negative for $|\Delta\eta| > 0.4$ and $|\Delta\eta| > 1.0$, which does not produce a real value of $v_3\{2\}$.³

³We also find that $c_3\{4\}$ only shows positive values, just as $c_2\{4\}$, which does not produce a real value of $v_3\{4\}$.

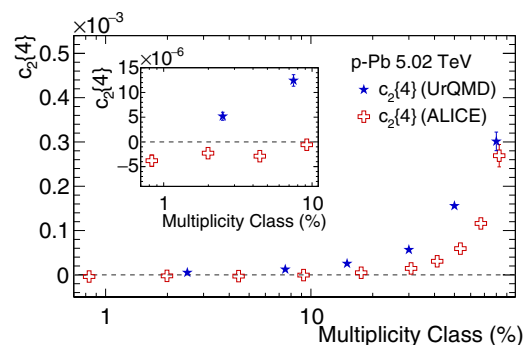


FIG. 4. (Color online) $c_2\{4\}$ of charged particles in p -Pb collisions at $\sqrt{s_{NN}} = 5.02$ TeV, calculated with UrQMD and measured by ALICE [42]. Here the multiplicity-class determination in UrQMD is based on Table I.

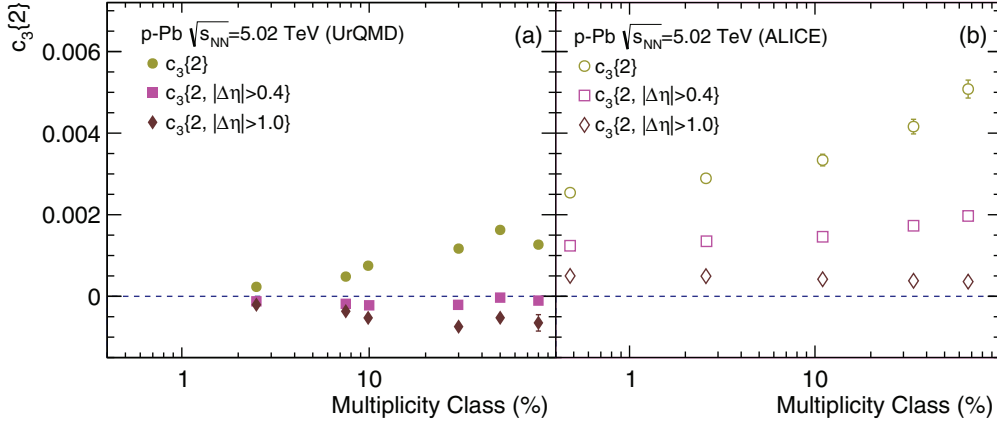


FIG. 5. (Color online) $c_3\{2\}$ of all charged hadrons in p -Pb collisions at $\sqrt{s_{NN}} = 5.02$ TeV, calculated UrQMD (left) and measured by ALICE (right) [42]. Here the multiplicity class determination in UrQMD is based on Table I.

The fact that UrQMD could not generate the experimentally observed triangular flow, together with the results shown Figs. 3–5, strongly indicates that p -Pb systems from UrQMD contain large non-flow azimuthal correlations.

Following Eq. (13), we calculate the second Fourier flow-coefficient as a function of transverse momentum $v_2(p_T)$ for the UrQMD simulations at multiplicity class 0%–20%, 20%–40%, 40%–60%, and 60%–100%. Figure 6 shows that $v_2(p_T)$ monotonically increases from high- to low-multiplicity class, which agrees with the trend of $c_2\{2\}$ shown in Fig. 3 ($c_2\{2\}$ is the square of the integrated $v_2\{2\}$). Meanwhile, $v_2(p_T)$ from UrQMD increases with the increase of p_T and shows strong sensitivity to the pseudorapidity gap. The observed large pseudorapidity-gap suppression of $v_2(p_T)$ indicates that non-flow effects are large in UrQMD, as already shown in Figs. 3–5.

Figure 6 also shows that UrQMD cannot correctly reproduce the shape of the experimental $v_2(p_T)$ curves when implemented with the same pseudorapidity gap $|\Delta\eta| > 1.0$. It underpredicts the data at lower p_T and overestimates the data above 1 GeV. Compared with the integrated v_2 , the differential elliptic flow $v_2(p_T)$ contains more information on the evolving system, which reflects the interplay between radial and elliptic flow. The m_T spectra in Fig. 2 has already shown that UrQMD cannot produce sufficient radial flow to reproduce the flow observed in experiment. The insufficient radial flow, together with the insufficient flow anisotropy accumulation (shown in Figs. 3–5) leads to the fact that UrQMD could not reproduce the $v_2(p_T)$ curves measured by ALICE.

Figure 7 investigates azimuthal correlations of identified hadrons in high-energy p -Pb collisions. The right panels present the ALICE measurements with two different multi-

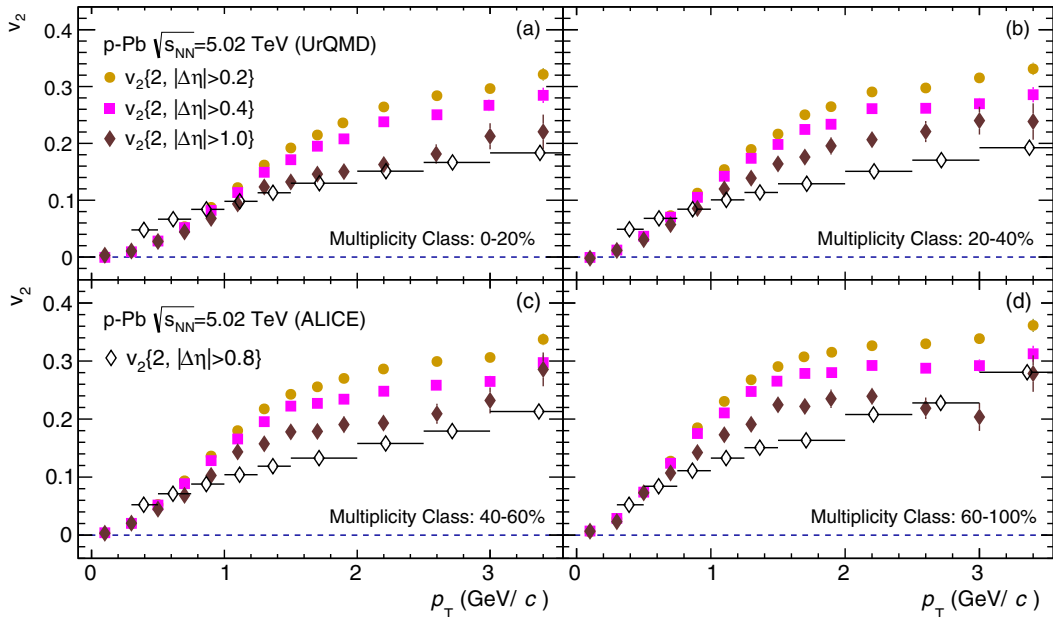


FIG. 6. (Color online) $v_2(p_T)$ of all change hadrons in p -Pb collisions at $\sqrt{s_{NN}} = 5.02$ TeV, calculated from UrQMD and measured by ALICE [43]. Here the multiplicity-class determination in UrQMD is based on Table II.

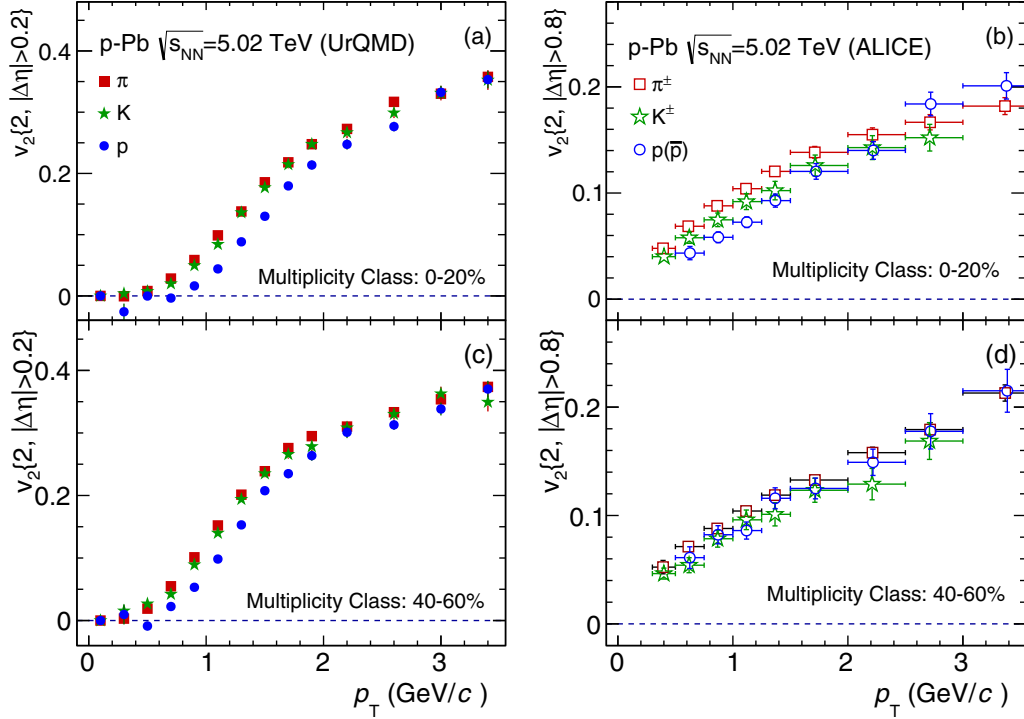


FIG. 7. (Color online) $v_2(p_T)$ of pions, kaons, and protons in p -Pb collisions at $\sqrt{s_{NN}} = 5.02$ TeV, calculated from UrQMD (left panels) and measured by ALICE (right panels) [43]. Here the multiplicity-class determination in UrQMD is based on Table II.

plicity classes [43,44], which show a characteristic feature of $v_2(p_T)$ mass ordering among pions, kaons, and protons. In past research, hydrodynamic simulations from several groups have systematically studied the flow data, which reproduced the v_2 mass-ordering feature of the p -Pb systems [46,49]. In hydrodynamic language, the radial flow further accumulated in the hadronic stage tends to push heavier hadrons from lower p_T to higher p_T , leading to an enhanced v_2 splitting between pions and protons [53,55]. The observation of v_2 mass ordering is thus generally believed as a strong evidence for the collective expansion of the p -Pb systems created in $\sqrt{s_{NN}} = 5.02$ TeV collisions.

However, the left panels of Fig. 7 shows that UrQMD also generate a mass-ordering for the two-particle correlations among pions, kaons, and protons.⁴ Such mass-ordering pattern, caused by pure hadronic interactions, qualitatively agrees with those from the ALICE measurement [43] and from the hydrodynamic calculations [46,49]. In UrQMD, the

⁴Due to limited statistics, we apply $|\Delta\eta| > 0.2$ in our calculations rather than $|\Delta\eta| > 0.8$ as used in experiment. In fact, $v_2\{2; |\Delta\eta| > 0.8\}$ from our current UrQMD simulations has large error bars, especially for protons. However, a tendency of v_2 mass ordering among pions, kaons, and protons is still observed.

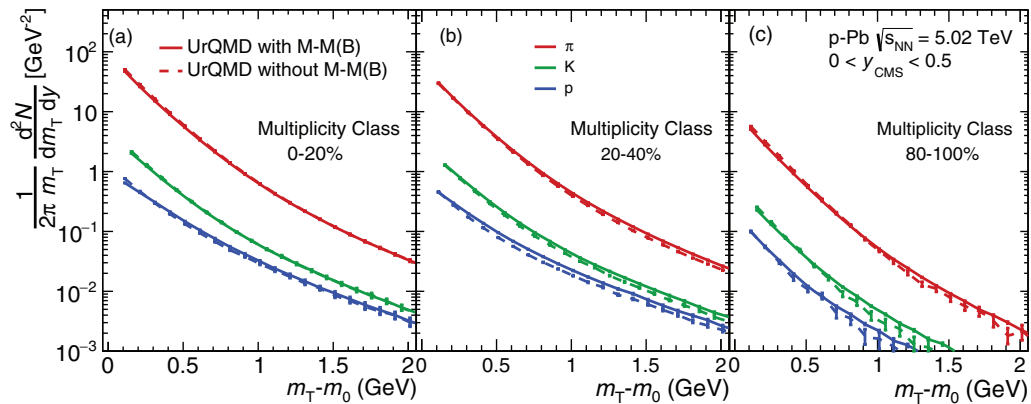


FIG. 8. (Color online) The m_T spectra of pions, kaons, and protons in p -Pb collisions at $\sqrt{s_{NN}} = 5.02$ TeV, calculated from UrQMD with and without M-M and M-B collisions. Here the multiplicity-class determination in UrQMD is based on Table II.

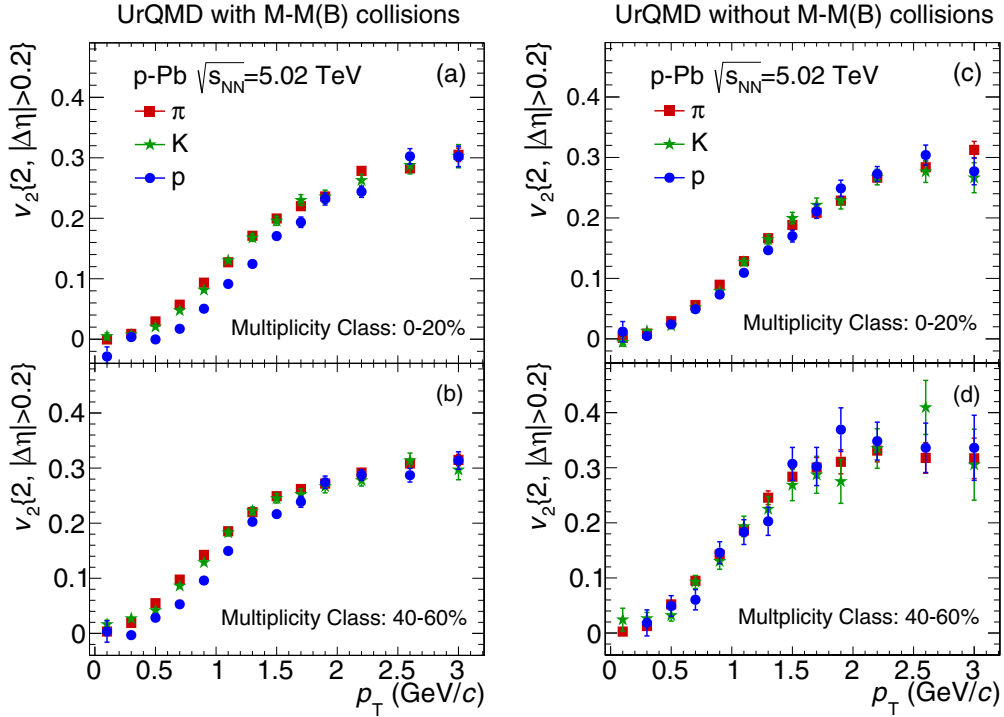


FIG. 9. (Color online) $v_2(p_T)$ of pions, kaons, and protons in p -Pb collisions at $\sqrt{s_{NN}} = 5.02$ TeV, calculated from UrQMD with and without M-M and M-B collisions. Here the multiplicity-class determination in UrQMD is based on Table II.

unknown cross sections are calculated by the additive quark model (AQM) through counting the number of constituent quarks within two colliding hadrons. As a result, the main meson-baryon (M-B) cross sections from AQM are about 50% larger than the meson-meson (M-M) cross sections, leading to the v_2 splitting between mesons and baryons after the evolution of hadronic matter. Comparison simulations in Appendix (Fig. 9) also show that, with the M-B and M-M interaction channels closed in UrQMD, the v_2 mass ordering almost disappears. The combined results in Figs. 7 and 9 illustrate that the hadronic interactions could lead to a mass-ordering in two-particle correlations among pions, kaons, and protons, even for small p -Pb systems without sufficient flow generation.

V. SUMMARY

By using the UrQMD hadron cascade model, we studied azimuthal correlations in p -Pb collisions at $\sqrt{s_{NN}} = 5.02$ TeV. Comparisons with the experimental data showed that the p -Pb systems created in experiment are not the trivial hadronic systems described by UrQMD. Here, we summarize the main results:

- (i) With large pseudorapidity gaps ($|\Delta\eta| > 1.0$), the measured two-particle cumulant of the second Fourier flow coefficient $c_2\{2\}$ from ALICE shows a weak centrality dependence from central to semiperipheral collisions. In contrast, the UrQMD calculations still present a strong centrality dependence for $c_2\{2, |\Delta\eta| > 1.0\}$.
- (ii) In the most-central collisions, $c_2\{4\}$ from ALICE exhibits a transition from positive to negative values, which indicates the development of strong collective

flow in high-multiplicity events. However, $c_2\{4\}$ from UrQMD keeps positive for all multiplicity classes, which does not produce $v_2\{4\}$ with a real value.

- (iii) For large pseudorapidity gaps, $c_3\{2\}$ from UrQMD becomes negative, which cannot produce the triangular flow as observed in experiments.
- (iv) UrQMD cannot fit the differential flow $v_2(p_T)$ from ALICE at various multiplicity classes.

More specifically, the related experimental data of azimuthal correlations have accumulated strong evidence for the development of strong collective flow in high-multiplicity events. With the assumption that high-energy p -Pb collisions do not reach the threshold for the QGP formation and only produce trivial hadronic systems, we did hadron transport simulations with UrQMD. We found that hadronic interactions alone could not generate sufficient collective flow to reproduce that observed in experiment. Non-flow effects, e.g., from resonance decays and/or jet-like fragmentations, largely influence the hadron emissions of the UrQMD systems. In order to fit the measured azimuthal correlations of all charged hadrons in p -Pb collisions at $\sqrt{s_{NN}} = 5.02$ TeV, the contributions from the initial stage and/or the QGP phase cannot be neglected.

In addition, we extended our study of azimuthal correlations to identified hadrons. The calculations of the two-particle correlations for pions, kaons, and protons showed that UrQMD can generate a v_2 mass ordering with the characteristic feature similar to the ALICE measurements. Comparison runs from UrQMD with main hadronic scatterings turned on and off showed that the v_2 mass ordering in UrQMD is mainly caused by hadronic interactions. The v_2 mass ordering alone is not

necessarily a flow signature associated with strong fluid-like expansions.

ACKNOWLEDGMENTS

We thank S. A. Bass, A. Bilandžić, J. J. Gaardhøje, U. Heinz, J. Y. Ollitrault, H. Petersen, J. Schukraft, and R. Snellings for valuable discussions. Y.Z. thanks to the Danish Council for Independent Research, Natural Sciences and the Danish National Research Foundation (Danmarks Grundforskningsfond) for support, thanks to Peking University for the host. X.Z., P.L., and H.S. are supported by the NSFC and the MOST under Grants No. 11435001 and No. 2015CB856900. We gratefully acknowledge the extensive computing resources provided to us on Tianhe-1A by the National Supercomputing Center in Tianjin, China.

APPENDIX: URQMD COMPARISON RUNS WITH AND WITHOUT M-M AND M-B COLLISIONS

This Appendix explores how hadronic interactions in UrQMD influence spectra and azimuthal correlations of identified hadrons for the hadronic p -Pb systems. In UrQMD, hadronic scatterings include meson-meson (M-M) collisions, meson-baryon (M-B) collisions, and baryon-baryon (B-B) collisions. When switching off all of these collision channels, UrQMD simulations, in principle, consist of initial hadron productions and the succeeding resonance decays, which are mainly influenced by non-flow effects. However, not all of these collision channels in the current version of UrQMD (v3.4) can be simultaneously turned off. With B-B collision channels turned off, all of the secondary proton-nucleon collisions from the initial p -Pb collisions are automatically turned off without proceeding any further hadron productions and decays. Considering that the probability of B-B collisions is much lower than that of M-M and M-B collisions, we only turn off the M-M and M-B interaction channels for the UrQMD comparison runs in this Appendix.

Figure 8 plots the m_T spectra of pions, kaons, and protons in p -Pb collisions at $\sqrt{s_{NN}} = 5.02$ TeV, calculated from UrQMD

with and without M-M and M-B interactions. In Sec. IV, we showed that, although the m_T scaling is weakly broken in UrQMD, pure hadronic interactions cannot generate sufficient radial flow to reproduce that observed in experiment. Here, Fig. 8 shows that M-M and M-B collisions only slightly change the slope of the m_T spectra.⁵ The slight breaking of the m_T scaling in UrQMD is very possibly caused by mechanisms of the initial hadron production.⁶

Compared with the m_T spectra, the v_2 mass ordering is more sensitive to hadronic interactions. For typical flow-dominated systems created in high-energy Au-Au or Pb-Pb collisions, hybrid model simulations show that hadronic rescatterings dramatically increase the v_2 splitting between pions and protons, but only slightly change the m_T spectra [54]. Figure 9 presents $v_2(p_T)$ of identified hadrons in high-energy p -Pb collisions, based on UrQMD simulations in the scenarios with (left panels) and without (right panels) M-M and M-B collisions. In the cases that M-M and M-B collisions are turned off, the v_2 mass ordering among pions, kaons, and protons almost disappears when compared with the cases with M-M and M-B interactions.

In Sec. IV, a detailed study of the two-particle and four-particle correlations has already shown that UrQMD could not generate sufficient flow to reproduce that observed in experiments; its final hadron emissions are largely influenced by non-flow effects. The comparison runs in Fig. 9 illustrate that the v_2 mass ordering can be explained as the consequence of hadronic interactions, which is not necessarily associated with strong fluid-like expansions.

⁵For 2.76A TeV Pb + Pb collisions at 70%–80% centrality (where $dN_{ch}/d\eta$ at midrapidity is about 50 [55] and close to $dN_{ch}/d\eta$ in high-multiplicity p -Pb collisions), hybrid model simulations also show that hadronic scatterings almost do not change the m_T spectra of identified hadrons [72].

⁶In the UrQMD simulations for p -Pb collisions at $\sqrt{s_{NN}} = 5.02$ TeV, most of the initial hadron productions are triggered by the PYTHIA mode due to large momentum transfer [56–58,73]. Backup simulations from PYTHIA with collision energy set to 5.02 TeV show that the m_T scaling is also weakly broken for the m_T spectra of pions, kaons, and protons [72].

-
- [1] I. Arsene *et al.* (BRAHMS Collaboration), *Nucl. Phys. A* **757**, 1 (2005); B. B. Back *et al.*, *ibid.* **757**, 28 (2005); J. Adams *et al.*, *ibid.* **757**, 102 (2005); K. Adcox *et al.*, *ibid.* **757**, 184 (2005).
 - [2] M. Gyulassy, in *Structure and Dynamics of Elementary Matter*, NATO science series II: Mathematics, Physics, and Chemistry, Vol. 166, edited by W. Greiner *et al.* (Kluwer Academic, Dordrecht, 2004), pp. 159–182; M. Gyulassy and L. McLerran, *Nucl. Phys. A* **750**, 30 (2005); E. V. Shuryak, *ibid.* **750**, 64 (2005).
 - [3] B. Muller and J. L. Nagle, *Annu. Rev. Nucl. Part. Sci.* **56**, 93 (2006).
 - [4] B. Muller, J. Schukraft, and B. Wyslouch, *Annu. Rev. Nucl. Part. Sci.* **62**, 361 (2012).
 - [5] J.-Y. Ollitrault, *Phys. Rev. D* **46**, 229 (1992).
 - [6] P. Huovinen, in *Quark Gluon Plasma 3*, edited by R. C. Hwa and X. N. Wang (World Scientific, Singapore, 2004), p. 600; P. F. Kolb and U. Heinz, *ibid.*, p. 634.
 - [7] D. A. Teaney, *arXiv:0905.2433*.
 - [8] P. Romatschke, *Int. J. Mod. Phys. E* **19**, 1 (2010).
 - [9] C. Gale, S. Jeon, and B. Schenke, *Int. J. Mod. Phys. A* **28**, 1340011 (2013).
 - [10] U. Heinz and R. Snellings, *Annu. Rev. Nucl. Part. Sci.* **63**, 123 (2013).
 - [11] H. Song, *Nucl. Phys. A* **904-905**, 114c (2013).
 - [12] S. Voloshin and Y. Zhang, *Z. Phys. C: Part. Fields* **70**, 665 (1996).

- [13] C. Alt *et al.* (NA49 Collaboration), *Phys. Rev. C* **68**, 034903 (2003).
- [14] K. H. Ackermann *et al.* (STAR Collaboration), *Phys. Rev. Lett.* **86**, 402 (2001); C. Adler *et al.*, *ibid.* **87**, 182301 (2001); *Phys. Rev. C* **66**, 034904 (2002).
- [15] J. Adams *et al.* (STAR Collaboration), *Phys. Rev. C* **72**, 014904 (2005); B. I. Abelev *et al.*, *ibid.* **77**, 054901 (2008); J. Adams *et al.*, *Phys. Rev. Lett.* **95**, 122301 (2005).
- [16] L. Adamczyk *et al.* (STAR Collaboration), *Phys. Rev. C* **88**, 014902 (2013).
- [17] K. Adcox *et al.* (PHENIX Collaboration), *Phys. Rev. Lett.* **89**, 212301 (2002); S. S. Adler *et al.*, *ibid.* **91**, 182301 (2003).
- [18] K. Aamodt *et al.* (ALICE Collaboration), *Phys. Rev. Lett.* **105**, 252302 (2010).
- [19] B. B. Abelev *et al.* (ALICE Collaboration), arXiv:1405.4632.
- [20] G. Aad *et al.* (ATLAS Collaboration), *Phys. Lett. B* **707**, 330 (2012).
- [21] S. A. Voloshin, A. M. Poskanzer, and R. Snellings, in *Relativistic Heavy Ion Physics*, edited by R. Stock (Springer-Verlag, Berlin, 2010), Vol. 23, pp. 5–54.
- [22] R. Snellings, *New J. Phys.* **13**, 055008 (2011).
- [23] B. Alver and G. Roland, *Phys. Rev. C* **81**, 054905 (2010); **82**, 039903 (2010).
- [24] R. S. Bhalerao, M. Luzum, and J. Y. Ollitrault, *Phys. Rev. C* **84**, 034910 (2011); **84**, 054901 (2011); F. G. Gardim, F. Grassi, M. Luzum, and J. Y. Ollitrault, *ibid.* **85**, 024908 (2012).
- [25] M. Luzum and H. Petersen, *J. Phys. G* **41**, 063102 (2014).
- [26] H. Petersen, G. Y. Qin, S. A. Bass, and B. Muller, *Phys. Rev. C* **82**, 041901 (2010); G. Y. Qin, H. Petersen, S. A. Bass, and B. Muller, *ibid.* **82**, 064903 (2010).
- [27] H. Holopainen, H. Niemi, and K. J. Eskola, *Phys. Rev. C* **83**, 034901 (2011).
- [28] L. Pang, Q. Wang, and X.-N. Wang, *Phys. Rev. C* **86**, 024911 (2012).
- [29] D. Teaney and L. Yan, *Phys. Rev. C* **86**, 044908 (2012).
- [30] B. Schenke, P. Tribedy, and R. Venugopalan, *Phys. Rev. C* **86**, 034908 (2012); C. Gale, S. Jeon, B. Schenke, P. Tribedy, and R. Venugopalan, *Phys. Rev. Lett.* **110**, 012302 (2013).
- [31] Z. Qiu and U. Heinz, *Phys. Lett. B* **717**, 261 (2012).
- [32] E. Retinskaya, M. Luzum, and J. Y. Ollitrault, *Phys. Rev. C* **89**, 014902 (2014).
- [33] K. Aamodt *et al.* (ALICE Collaboration), *Phys. Rev. Lett.* **107**, 032301 (2011); *Phys. Lett. B* **708**, 249 (2012).
- [34] G. Aad *et al.* (ATLAS Collaboration), *Phys. Rev. C* **86**, 014907 (2012).
- [35] S. Chatrchyan *et al.* (CMS Collaboration), *Eur. Phys. J. C* **72**, 2012 (2012).
- [36] L. Adamczyk *et al.* (STAR Collaboration), *Phys. Rev. C* **88**, 014904 (2013).
- [37] A. Adare *et al.* (PHENIX Collaboration), *Phys. Rev. Lett.* **107**, 252301 (2011).
- [38] B. Abelev *et al.* (ALICE Collaboration), *Phys. Lett. B* **719**, 29 (2013).
- [39] R. S. Bhalerao, N. Borghini, and J. Y. Ollitrault, *Nucl. Phys. A* **727**, 373 (2003).
- [40] Q. Wang (CMS Collaboration), *Nucl. Phys. A* **931**, 997 (2014).
- [41] G. Aad *et al.* (ATLAS Collaboration), *Phys. Lett. B* **725**, 60 (2013).
- [42] B. B. Abelev *et al.* (ALICE Collaboration), *Phys. Rev. C* **90**, 054901 (2014).
- [43] B. B. Abelev *et al.* (ALICE Collaboration), *Phys. Lett. B* **726**, 164 (2013).
- [44] V. Khachatryan *et al.* (CMS Collaboration), *Phys. Lett. B* **742**, 200 (2015).
- [45] P. Bozek and W. Broniowski, *Phys. Lett. B* **718**, 1557 (2013); P. Bozek, *Phys. Rev. C* **85**, 014911 (2012); P. Bozek and W. Broniowski, *ibid.* **88**, 014903 (2013).
- [46] P. Bozek, W. Broniowski, and G. Torrieri, *Phys. Rev. Lett.* **111**, 172303 (2013).
- [47] A. Bzdak, B. Schenke, P. Tribedy, and R. Venugopalan, *Phys. Rev. C* **87**, 064906 (2013).
- [48] G.-Y. Qin and B. Müller, *Phys. Rev. C* **89**, 044902 (2014).
- [49] K. Werner, M. Bleicher, B. Guiot, I. Karpenko, and T. Pierog, *Phys. Rev. Lett.* **112**, 232301 (2014).
- [50] P. F. Kolb, J. Sollfrank, and U. W. Heinz, *Phys. Rev. C* **62**, 054909 (2000).
- [51] H. Song and U. W. Heinz, *Phys. Rev. C* **77**, 064901 (2008).
- [52] C. Nonaka and S. A. Bass, *Phys. Rev. C* **75**, 014902 (2007).
- [53] T. Hirano, U. W. Heinz, D. Kharzeev, R. Lacey, and Y. Nara, *Phys. Rev. C* **77**, 044909 (2008).
- [54] H. Song, S. A. Bass, and U. Heinz, *Phys. Rev. C* **83**, 024912 (2011).
- [55] H. Song, S. A. Bass, and U. Heinz, *Phys. Rev. C* **89**, 034919 (2014); X. Zhu, F. Meng, H. Song, and Y. X. Liu, *ibid.* **91**, 034904 (2015).
- [56] S. A. Bass *et al.*, *Prog. Part. Nucl. Phys.* **41**, 255 (1998).
- [57] M. Bleicher *et al.*, *J. Phys. G* **25**, 1859 (1999).
- [58] H. Petersen, M. Bleicher, S. A. Bass, and H. Stocker, arXiv:0805.0567.
- [59] T. Sjostrand, L. Lonnblad, S. Mrenna, and P. Z. Skands, arXiv:hep-ph/0308153.
- [60] B. B. Abelev *et al.* (ALICE Collaboration), *Phys. Lett. B* **728**, 25 (2014).
- [61] B. Abelev *et al.* (ALICE Collaboration), *Phys. Rev. Lett.* **110**, 032301 (2013).
- [62] A. Bilandžić, R. Snellings, and S. Voloshin, *Phys. Rev. C* **83**, 044913 (2011).
- [63] A. Bilandžić, C. H. Christensen, K. Gulbrandsen, A. Hansen, and Y. Zhou, *Phys. Rev. C* **89**, 064904 (2014).
- [64] G. Agakishiev *et al.* (STAR Collaboration), *Phys. Rev. C* **86**, 014904 (2012).
- [65] Y. Zhou (ALICE Collaboration), *Nucl. Phys. A* **931**, 949 (2014).
- [66] U. W. Heinz, arXiv:hep-ph/0407360.
- [67] O. Y. Barannikova *et al.* (STAR Collaboration), *Nucl. Phys. A* **715**, 458 (2003).
- [68] S. V. Afanasiev *et al.*, *Nucl. Phys. A* **715**, 161 (2003).
- [69] J. Velkovska (PHENIX Collaboration), *Nucl. Phys. A* **698**, 507 (2002); K. Adcox *et al.*, *Phys. Rev. Lett.* **88**, 242301 (2002).
- [70] C. Adler *et al.* (STAR Collaboration), *Phys. Rev. Lett.* **87**, 262302 (2001).
- [71] E. Schnedermann, J. Sollfrank, and U. Heinz, *Phys. Rev. C* **48**, 2462 (1993).
- [72] X. R. Zhu and H. Song (unpublished).
- [73] S. A. Bass (private communication).